RESEARCH BRIEF

Metabolic and Functional Genomic Studies Identify Deoxythymidylate Kinase as a Target in *LKB1*-Mutant Lung Cancer

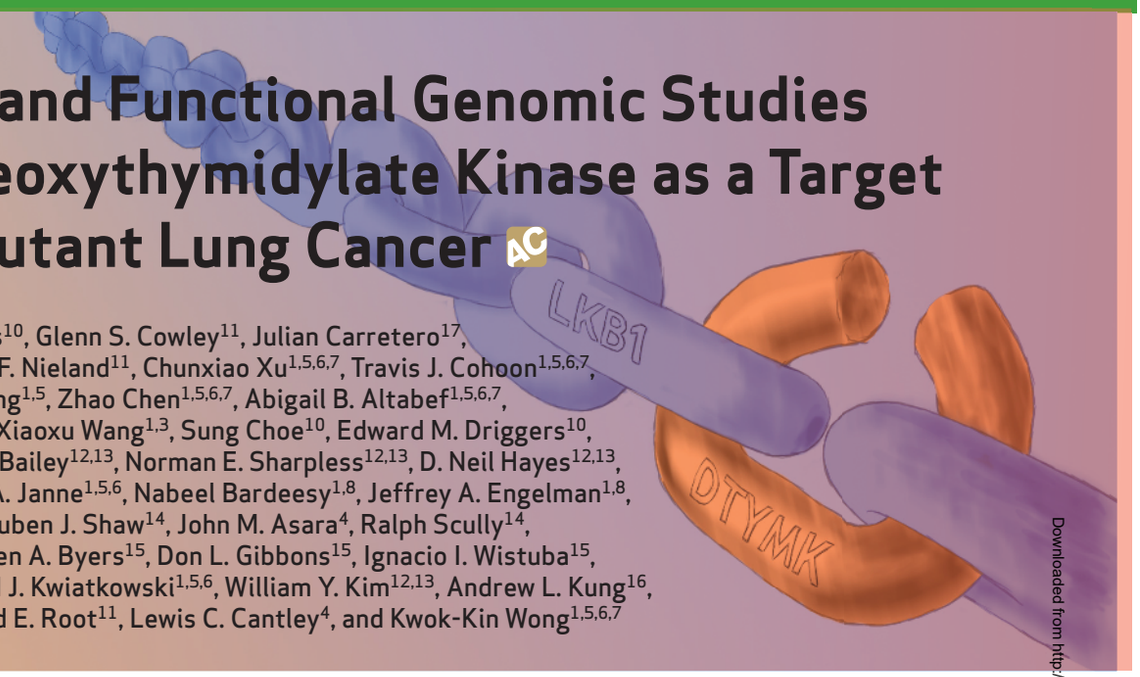

Yan Liu[1,5,6,7], Kevin Marks[10], Glenn S. Cowley[11], Julian Carretero[17], Qingsong Liu[2], Thomas J.F. Nieland[11], Chunxiao Xu[1,5,6,7], Travis J. Cohoon[1,5,6,7], Peng Gao[1,5,6,7], Yong Zhang[1,5], Zhao Chen[1,5,6,7], Abigail B. Altabef[1,5,6,7], Jeremy H. Tchaicha[1,5,6,7], Xiaoxu Wang[1,3], Sung Choe[10], Edward M. Driggers[10], Jianming Zhang[2], Sean T. Bailey[12,13], Norman E. Sharpless[12,13], D. Neil Hayes[12,13], Nirali M. Patel[12,13], Pasi A. Janne[1,5,6], Nabeel Bardeesy[1,8], Jeffrey A. Engelman[1,8], Brendan D. Manning[9], Reuben J. Shaw[14], John M. Asara[4], Ralph Scully[14], Alec Kimmelman[1,3], Lauren A. Byers[15], Don L. Gibbons[15], Ignacio I. Wistuba[15], John V. Heymach[15], David J. Kwiatkowski[1,5,6], William Y. Kim[12,13], Andrew L. Kung[16], Nathanael S. Gray[2], David E. Root[11], Lewis C. Cantley[4], and Kwok-Kin Wong[1,5,6,7]

ABSTRACT

The *LKB1/STK11* tumor suppressor encodes a serine/threonine kinase, which coordinates cell growth, polarity, motility, and metabolism. In non–small cell lung carcinoma, *LKB1* is somatically inactivated in 25% to 30% of cases, often concurrently with activating *KRAS* mutations. Here, we used an integrative approach to define novel therapeutic targets in KRAS-driven *LKB1*-mutant lung cancers. High-throughput RNA interference screens in lung cancer cell lines from genetically engineered mouse models driven by activated KRAS with or without coincident *Lkb1* deletion led to the identification of *Dtymk*, encoding deoxythymidylate kinase (DTYMK), which catalyzes dTTP biosynthesis, as synthetically lethal with *Lkb1* deficiency in mouse and human lung cancer lines. Global metabolite profiling showed that *Lkb1*-null cells had a striking decrease in multiple nucleotide metabolites as compared with the *Lkb1*–wild-type cells. Thus, *LKB1*-mutant lung cancers have deficits in nucleotide metabolism that confer hypersensitivity to DTYMK inhibition, suggesting that DTYMK is a potential therapeutic target in this aggressive subset of tumors.

SIGNIFICANCE: Using cell lines derived from the lung cancers occurring in genetically engineered mice, we conducted an integrative genome-wide short hairpin RNA and metabolite screen to identify *DTYMK* as a potential therapeutic target in *Kras/Lkb1*–mutant lung cancer. We believe that DTYMK is tractable for the development of novel therapeutics, and show an integrative approach to target identification that reduces false-positive candidates and should have broad applicability for the development of targeted therapeutics. *Cancer Discov; 3(8); 870–9. ©2013 AACR.*

See related commentary by Marcus and Khuri, p. 843.

Authors' Affiliations: Departments of [1]Medicine, [2]Biological Chemistry and Molecular Pharmacology, and [3]Radiation Oncology; [4]Department of Medicine, Beth Israel Deaconess Medical Center, Harvard Medical School; [5]Department of Medical Oncology; [6]Lowe Center for Thoracic Oncology; [7]Ludwig Center, Dana-Farber/Harvard Cancer Center; [8]Massachusetts General Hospital Cancer Center; [9]Department of Genetics and Complex Diseases, Harvard School of Public Health, Boston; [10]Agios Pharmaceuticals; [11]Broad Institute of MIT and Harvard, Cambridge, Massachusetts; [12]Lineberger Comprehensive Cancer Center; [13]Department of Medicine and Genetics, University of North Carolina at Chapel Hill, Chapel Hill, North Carolina; [14]Molecular and Cell Biology Laboratory, The Salk Institute for Biological Studies, La Jolla, California; [15]The University of Texas MD Anderson Cancer Center, Houston, Texas; [16]Department of Pediatrics, Columbia University Medical Center, New York, New York; [17]Department of Physiology, University of Valencia, Burjassot, Spain

Note: Supplementary data for this article are available at Cancer Discovery Online (http://cancerdiscovery.aacrjournals.org/).

Corresponding Author: Kwok-Kin Wong, Dana-Farber Cancer Institute, Dana Building 810B, 450 Brookline Avenue, HIM243, Boston, MA 02115. Phone: 617-632-6084; Fax: 617-632-7839; E-mail: kwong1@partners.org

doi: 10.1158/2159-8290.CD-13-0015

INTRODUCTION

LKB1/STK11 functions as a master regulator of cell metabolism and energy stress responses (1, 2). Its best-characterized target is AMP-activated protein kinase (AMPK), which is directly phosphorylated and activated by LKB1 in the context of low cellular ATP levels (2). AMPK in turn modulates nutrient use to restore energy homeostasis through phosphorylation of multiple substrates controlling nutrient uptake and metabolism (1, 2). LKB1 also activates other members of the AMPK-related family of kinases, which regulate diverse aspects of cell metabolism, growth, and polarity (1, 2). *LKB1/STK11* deficiency results in broad defects in metabolic control, as evidenced by primary cells and cancer cell lines lacking *LKB1* being sensitized to nutrient deprivation and other types of metabolic stress (3–5). *LKB1* is also a major tumor suppressor gene that is somatically inactivated in many common types of cancer (3, 4). Human tumor data and genetic studies in mice suggest that *LKB1*-mutant cancers are biologically distinct from those with LKB1 intact (6). Notably, *LKB1* inactivation is the single most prominent biomarker for poor outcome in cervical cancer, predicting survival of 1 year, as compared with 10-year survival for *LKB1* wild-type (WT) tumors (7). In mouse models of lung cancer and melanoma, *Lkb1* loss synergizes with active KRAS to drive a highly metastatic phenotype not seen in the context of other combinations of mutations (6, 8). Unfortunately, there are currently few drugs available for clinical use that target *LKB1* loss specifically, and recent human cancer cell line screens using more than 130 drugs under clinical and preclinical investigation failed to identify known anticancer agents with strong selective activity in this subset of tumors (data not shown; ref. 9).

Here, we sought to use an integrative program to systematically identify novel drug targets in *LKB1*-mutant lung cancer using a synthetic lethal RNA interference (RNAi) screen and comprehensive metabolomics analysis. For these studies, we took advantage of a series of low-passage lung cancer cell lines derived from genetically engineered mouse models (GEMM) programmed with common mutations in *Kras* and *Trp53*, alone or in combination with *Lkb1*. Although the heterogeneity of human cancer cell lines can obscure synthetic lethal associations, we predicted that this murine cell line panel, developed in the context of a well-defined model system, would effectively enable the discovery of genotype-driven sensitivities.

RESULTS

Generation of Lung Cancer Cell Lines from GEMMs

To generate isogenic lung cancer cell lines, somatic KRAS activation and *Trp53* loss with or without *Lkb1* inactivation were induced in the lungs of genetically engineered mice ($Kras^{+/LSL\text{-}G12D}Trp53^{L/L}$ or $Kras^{+/LSL\text{-}G12D}Trp53^{L/L}Lkb1^{L/L}$) by intranasal administration of Adenovirus-Cre as previously described (6). Inactivation of *Trp53* was included in these models, as inactivation of *Tp53* is common in human non–small cell lung carcinoma (NSCLC; >50%; ref. 10). Tumor nodules from mice of defined genotypes were dissected, minced, and cultured, resulting in the derivation of the 634, 855, and 857 lines from $Kras^{+/LSL\text{-}G12D}Trp53^{L/L}$ mice (*Lkb1*-WT) and the t2, t4, and t5 lines from $Kras^{+/LSL\text{-}G12D}Trp53^{L/L}Lkb1^{L/L}$ mice (*Lkb1*-null; Supplementary Fig. S1A). Genotype, LKB1 expression, and epithelial origin of the lines were confirmed by PCR, Western blot analysis, and pan-cytokeratin immunostaining (Supplementary Fig. S1B–S1D). These six lines showed similar growth rates (Supplementary Fig. S1E), and the *Lkb1*-null lines exhibited lower cellular ATP levels compared with *Lkb1*-WT cells (Supplementary Fig. S1F).

Identification of Selective Essential Genes in *Kras/Trp53/Lkb1* GEMM-Derived Cell Lines

To identify genes that induce cell death selectively in *Lkb1*-null lung cancers, a synthetic lethal screen was conducted using a pooled 40K murine short hairpin RNA (shRNA) lentiviral library with each of the *Lkb1*-WT and *Lkb1*-null cell lines. The relative abundance of shRNAs in each cell line sample was determined by deep-sequencing, and for every shRNA, a $\log_2$ fold change ($\log_2$FC) value was calculated from the difference in relative abundance at a late time point after infection versus the initial shRNA-infected sample. Unsupervised hierarchical clustering analysis of the ranked hairpins from the triplicate pooled shRNA library screens revealed clear clustering of the *Lkb1*-WT and *Lkb1*-null cells into distinct groups, and the blue color in the top right corner represents genes for which the abundance of shRNAs is significantly reduced in all *Lkb1*-null cultures, suggesting a specific effect in the inhibition of *Lkb1*-null cell growth (Fig. 1A). We collapsed the ranked hairpins using two methods, a RIGER analysis (Kolmogorov–Smirnov *t* test–based statistics) and a weighted second-best analysis to rank genes that selectively impaired proliferation/viability in *Lkb1*-null cells. We nominated a union of 344 genes, identified by the top 100 individual hairpins for 88 genes (Supplementary Table S1.1) and the top 200 genes from both the Kolmogorov–Smirnov (Supplementary Table S1.2) and weighted second-best analysis (Supplementary Table S1.3), as our initial prioritized list (Fig. 1B). Of note, 340 shRNAs, targeting 70 candidate genes from this prioritized list, were chosen for validation (Supplementary Table S1.4). These 70 genes consisted of the top 10 candidates from the Kolmogorov–Smirnov analysis, as well as 60 others involved in a range of biologic processes in an attempt to represent all biologic categories in the validation process. Validation was conducted in an array format and identified 13 genes that displayed two or more hairpins with a significant growth disadvantage in the *Lkb1*-null cells (Supplementary Table S1.5). Deoxythymidylate kinase (*Dtymk*), *Chek1*, *Pdhb*, and *Cmpk1* were the top four candidates, each with two or more hairpins that scored in the validation assay (Fig. 1C and Supplementary Table S1.5).

Metabolomics Analysis Implicates *Dtymk* as a Critical Gene in *Lkb1*-Null Cells

LKB1 is reported to be involved in metabolic reprogramming (4, 11); therefore, we assessed the metabolic profile of *Lkb1*-WT and *Lkb1*-null cells and discovered a set of 58 metabolites, including the nucleotide metabolites IMP, AMP, ADP, GMP, dGMP, UMP, UDP, CDP, dCDP, and dTDP, which were present at consistently lower levels in *Lkb1*-null cells (Fig. 1D). Pathway enrichment analysis showed that metabolites in both purine and pyrimidine metabolism were significantly reduced in *Lkb1*-null compared with *Lkb1*-WT cells (Fig. 1D; $P = 3.5 \times 10^{-7}$ and 3.4×10^{-5}, respectively), including multiple metabolites involved in dTTP synthesis, such as dTDP

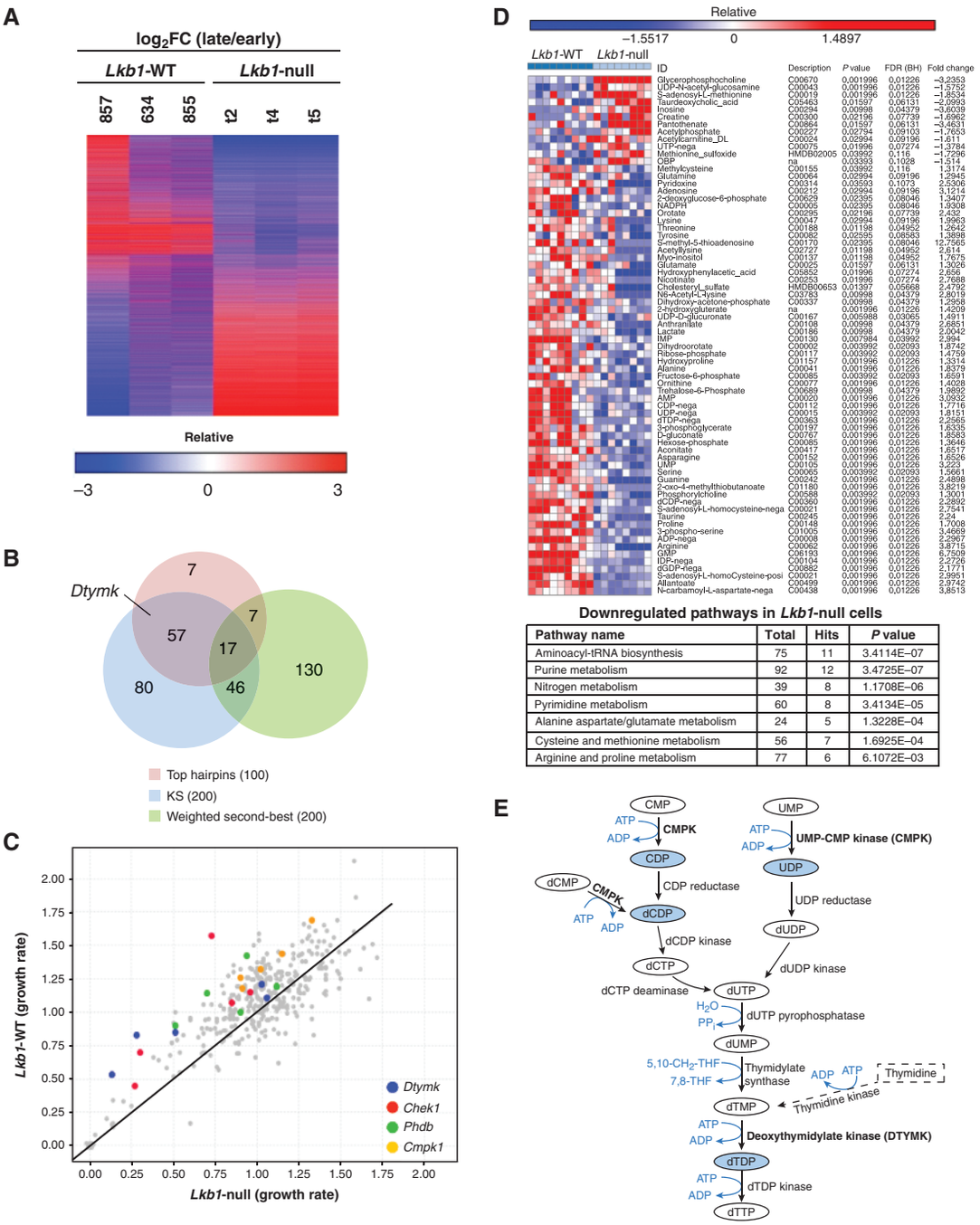

Figure 1. Identifying *Dtymk*. **A,** unsupervised hierarchical clustering analysis of results from triplicate pooled shRNA library screens of *Lkb1*-WT and *Lkb1*-null mouse cancer cell lines based on $\log_2$FC. Negative numbers (blue) reflect relative depletion of shRNAs at late time points. **B,** two-class comparison of *Lkb1*-null versus *Lkb1*-WT cell lines was used to generate a ranked hairpin list of selectively essential hairpins in an *Lkb1*-null background. Hairpins were collapsed to gene values using either the weighted second-best or the Kolmogorov–Smirnov (KS) statistic in GENE-E. Venn diagram depicts the overlap of most essential genes in the *Lkb1*-null background nominated by the top 100 independent hairpins, and the top 200 genes from both weighted second-best and KS. **C,** validation study. Relative viability of *Lkb1*-WT and *Lkb1*-null cells infected with 340 individual hairpins for 5 days. Genes of interest are highlighted by the colors indicated. **D,** metabolic signature of *Lkb1*-null lung cancer cells. Unsupervised clustering analysis of metabolomic data from *Lkb1*-WT and *Lkb1*-null cells. The heatmap displays those metabolites with the greatest difference between *Lkb1*-WT and *Lkb1*-null cell lines, along with compound name (ID), description (KEGG identification number), and *P* value, etc., for comparison between the two sets of lines. Bottom, significantly enriched metabolic pathways in downregulated components of the *Lkb1*-null metabolic signature using the pathway analysis module from the MetaboAnalyst tool (http://www.metaboanalyst.ca). **E,** a comprehensive metabolic map of the *de novo* (solid line) and the salvage (dashed line) pyrimidine deoxyribonucleotide biosynthetic pathway. This map was created with CellDesigner version 4.2 using a template from the Panther Classification System Database (www.pantherdb.org). DTYMK is highlighted in bold. Metabolites depicted in light blue were significantly downregulated in *Lkb1*-null cells.

(the product of DTYMK) and UDP/CDP/dCDP (products of UMP-CMP kinase; Fig. 1E; refs. 12, 13). Collectively, these two independent sets of data suggest that *Lkb1*-mutant lung cancer cells exhibit alterations in dTTP metabolism and are particularly sensitized to disruption of intracellular dTTP synthesis, and therefore have potential as important targets in *Lkb1*-null lung cancer.

Dtymk Is a Synthetic Lethal Gene Selectively Required for *Lkb1*-Null Cell Proliferation

To further examine the role of DTYMK in lung tumorigenesis, we screened five sh*Dtymk*s and identified sh*Dtymk-1* and sh*Dtymk-3*, which knocked down *DTYMK* to nearly undetectable levels (Supplementary Fig. S2A and Supplementary Table S2). Compared with sh*GFP*, both sh*Dtymk-1* and sh*Dtymk-3* strongly inhibited the growth of the *Lkb1*-null cells (t2, t4, and t5), while producing a weaker effect in the *Lkb1*-WT (634, 855, and 857) cell lines (Fig. 2A and Supplementary Fig. S2B). To see if overexpression of shRNA-resistant *Dtymk* can rescue the sh*Dtymk* effect, *Dtymk-R1* and *Dtymk-R3* were cloned into the pLenti6 vector and then transduced into *Lkb1*-null t4 cells. Blasticidin-resistant cells were pooled and further transduced with sh*GFP*, sh*Dtymk-1*, or sh*Dtymk-3*, respectively. Consistently, sh*Dtymk-1* and sh*Dtymk-3* killed *Lkb1*-null t4 cells within 3 days, whereas *Dtymk-R1* and *Dtymk-R3* expression largely restored the growth of sh*Dtymk-1*– and sh*Dtymk-3*–transduced t4 cells (Fig. 2B). Western blot analysis revealed lower DTYMK signals in t4-*Dtymk-R1*/sh*Dtymk-1* and t4-*Dtymk-R3/shDtymk-3* cells, suggesting that some of the blasticidin-resistant cells were not DTYMK-R–positive and thus were killed by sh*Dtymk* (Fig. 2B), which likely accounted for the significant but incomplete rescue by *Dtymk-R1* or *Dtymk-R3*. To extend these findings to tumorigenesis *in vivo*, *Lkb1*-WT (634 and 857) and *Lkb1*-null (t2 and t4) cells were transduced with doxycycline-inducible (TetOn) sh*GFP* or sh*Dtymk-3* and then implanted into athymic nude mice. Consistent with the *in vitro* proliferation assay, doxycycline-induced expression of sh*Dtymk-3* for 3 weeks resulted in a marked impairment in the growth of *Lkb1*-null tumors while producing more modest effects in the *Lkb1*-WT tumors (Fig. 2C).

Dtymk Knockdown Alters Pyrimidine Metabolism

DTYMK catalyzes the phosphorylation of dTMP to form dTDP, and it is the first merged step of both the *de novo* and salvage pathways in the production of dTTP (Fig. 1E). We expected that knockdown of *Dtymk* would inhibit this pathway and lead to accumulation of the substrate dTMP and a decrease in the product dTDP. Corresponding metabolite analysis of *Lkb1*-WT 634 and *Lkb1*-null t4 cells transduced with sh*Dtymk-1* revealed the expected significant increase in dTMP and moderate decrease in dTDP levels in both cell lines (Fig. 2D), indicating that DTYMK is a major source of dTDP in the cells and underscores the importance of this gene in cancer cell proliferation, as dTDP is required for production of dTTP for DNA synthesis.

dTTP Rescues the sh*Dtymk* Growth Phenotype

To investigate whether adding dTTP to the medium can rescue sh*Dtymk*-induced cell death, *Lkb1*-WT 634 and *Lkb1*-null t4 cell lines were transduced with sh*GFP*, sh*Dtymk-1*, or sh*Dtymk-3* and cultured in the presence or absence of 100 μmol/L dTTP for 4 days (14). Consistently, sh*Dtymk-1* and sh*Dtymk-3* killed more *Lkb1*-null t4 cells than *Lkb1*-WT 634 cells, but not the cells cultured in medium containing exogenous dTTP (Fig. 2E; confirmation of *Dtymk* knockdown and incorporation of the exogenous dTTP into DNA are shown in Supplementary Fig. S3A and S3B). Collectively, our data indicate that dNTP metabolism is impaired in *Lkb1*-deficient lung cancer cells, and that targeting *Dtymk* is synthetically lethal in this setting.

Lkb1-Null Cells Are More Prone to DNA Damage than *Lkb1*-WT Cells

Knockdown of *Dtymk* will consequently reduce dTTP but also increase dUTP levels. Such changes have been previously linked to dUTP misincorporation and DNA damage, when high expression levels of ribonucleotide reductase R2 subunit activate nucleotide excision repair (15–18). We noted that, although *Lkb1*-null and *Lkb1*-WT cells have similar R2 expression, *Lkb1*-null cells have much lower DTYMK expression (Fig. 3A), potentially creating a cellular state favorable for dUTP misincorporation. Supportively, *Lkb1*-null cells have a large 4N peak in DNA content (Fig. 3B), are more sensitive to CHEK1 inhibition (Fig. 3C and Supplementary Fig. S4A), and have slightly increased basal phospho-CHEK1 (Fig. 3A), consistent with the activation of a G_2 DNA damage checkpoint during replication in *Lkb1*-null cells (19–22). This pathway seems relevant *in vivo*. *Lkb1*-null tumors exhibited increased γH2AX and phospho-CHEK1 signals as compared with *Lkb1*-WT tumors (Supplementary Fig. S5A–S5C), suggesting there is more DNA damage *in vivo* than under *in vitro* culture conditions. In line with this evidence for more DNA damage in *Lkb1*-null cells, it is notable that *Chek1* ranked second in our screen (Fig. 1C and Supplementary Table S1.5), suggesting a dependence of *Lkb1*-null cell survival on CHEK1 function. Knockdown of *Dtymk* over a short period (i.e., 2.5 days after sh*Dtymk*-transduction) resulted in comparable increases in the phosphorylation of CHEK1 and H2AX in both cell types, whereas the phosphorylation of replication protein A 32 kDa subunit (RPA32) was much more pronounced in *Lkb1*-null cells (Fig. 3A), suggesting more DNA damage and elevation in nucleotide excision repair in *Lkb1*-null cells (23). Interestingly, the expression of total RPA32 was increased in *Lkb1*-WT cells (Fig. 3A), suggesting that LKB1 may positively regulate RPA32 expression following *Dtymk* knockdown and more DNA damage. Collectively, these data suggest that *Lkb1* loss sensitizes cells to DTYMK-depletion–induced DNA damage and replication stress, as equivalent knockdown of *Dtymk* in *Lkb1*-null and *Lkb1*-WT cells leads to more robust DNA damage in the *Lkb1*-null cell lines.

DNA Replication Is More Sensitive to *Dtymk* Knockdown in *Lkb1*-Null Cells than in *Lkb1*-WT Cells

To examine how the knockdown of *Dtymk* affects DNA synthesis, *Lkb1*-WT and *Lkb1*-null cells were pulse-labeled with 5-iododeoxyuridine (IdU) for 20 minutes at 0, 2.5, and 3.5 days posttransduction with sh*Dtymk-1*. As shown in Fig. 3D,

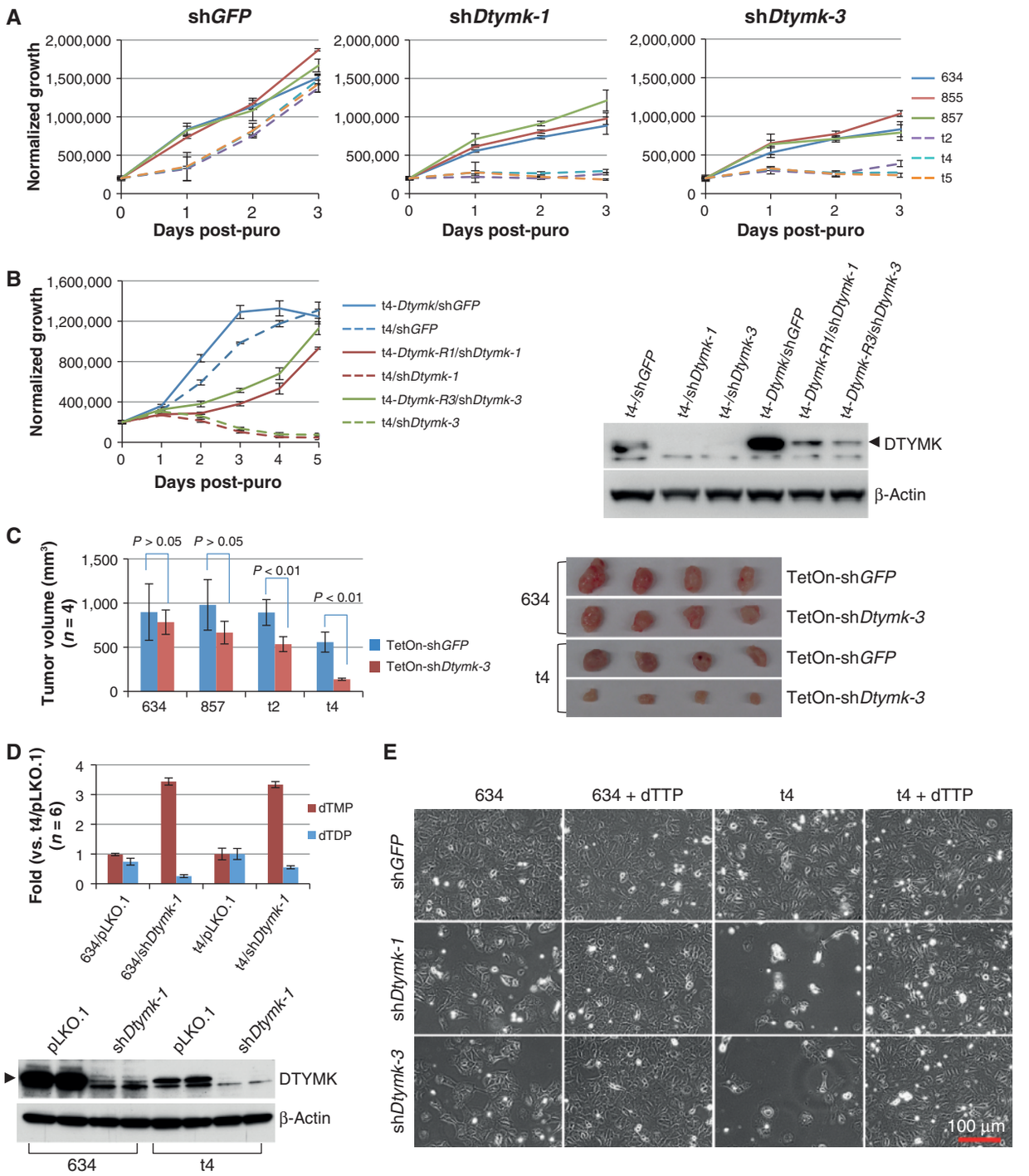

Figure 2. *Dtymk* is a synthetic lethal target of *Lkb1* loss. **A,** *Lkb1*-WT (634, 855, and 857) and *Lkb1*-null (t2, t4, and t5) cells were transduced with the indicated shRNA for 2 days and then plated into 96-well plates at 2,000 cells per well in 150 μL medium with 3 μg/mL puromycin (puro). Viable cells were measured daily using Promega's CellTiter-Glo Assay. The data represent mean ± SD for three replicates. **B,** *Lkb1*-null t4 cells were first transduced with pLenti6-*Dtymk*, pLenti6-*Dtymk-R1*, or pLenti6-*Dtymk-R3*, and selected with blasticidin. The blasticidin-resistant cells were pooled and further transduced with the indicated shRNA for 2 days and then plated for proliferation assay as described in **A**. The data represent mean ± SD for three replicates. **C,** a total of 1×10^6 *Lkb1*-WT (634 and 857) and *Lkb1*-null (t2 and t4) cells transduced with the indicated shRNA were implanted into athymic nude mice for 3 weeks. Tumor volume (mm^3) was calculated as (length × width^2)/2. The data represent mean ± SD for four mice. *Lkb1*-WT 634 and *Lkb1*-null t4 tumors with the indicated shRNAs are shown. **D,** graph of dTMP and dTDP levels in *Lkb1*-WT 634 and *Lkb1*-null t4 cells transduced with the indicated shRNA for 3 days. The data represent mean ± SD for six replicates. Expression of DTYMK in these cells at the time of metabolite extraction was determined by Western blotting. **E,** morphology of *Lkb1*-WT 634 and *Lkb1*-null t4 cells transduced with the indicated shRNA and then cultured in medium with or without additional 100 μmol/L dTTP for 4 days.

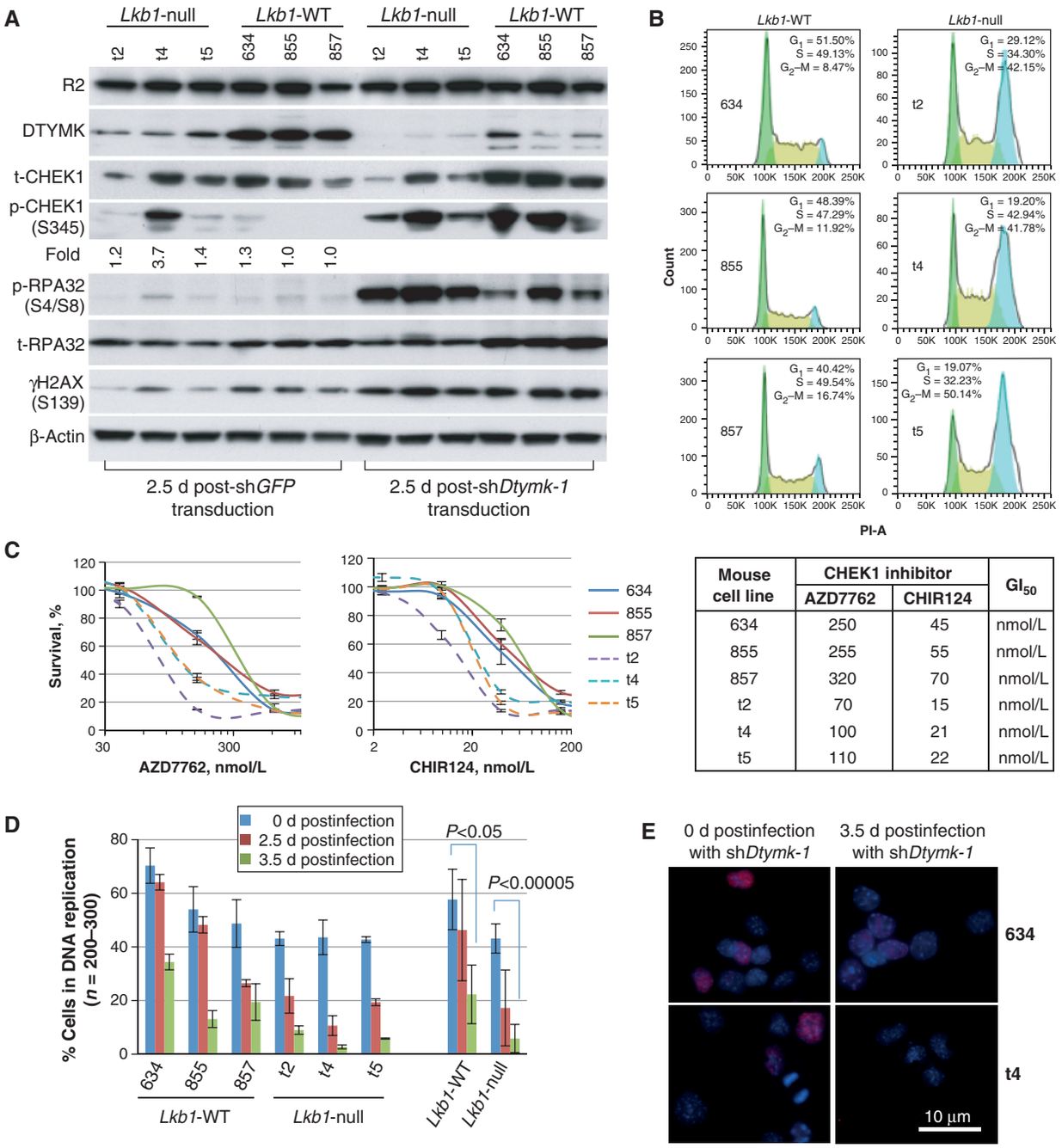

Mouse cell line	CHEK1 inhibitor		GI_{50}
	AZD7762	CHIR124	
634	250	45	nmol/L
855	255	55	nmol/L
857	320	70	nmol/L
t2	70	15	nmol/L
t4	100	21	nmol/L
t5	110	22	nmol/L

Figure 3. Characterization of *Lkb1*-WT and *Lkb1*-null cell lines. **A,** Western blot analyses of the indicated protein expression in *Lkb1*-WT (634, 855, and 857) and *Lkb1*-null (t2, t4, and t5) cell lines after *Dtymk-1* knockdown. Phospho-CHEK1 Western blot analysis bands were quantified by ImageJ. **B,** *Lkb1*-WT (634, 855, and 857) and *Lkb1*-null (t2, t4, and t5) cell lines in log-phase growth were fixed with cold 70% ethanol, stained with propidium iodide (PI), and then analyzed with flow cytometry; 20,000 cells per line were analyzed. **C,** *Lkb1*-WT (634, 855, and 857) and *Lkb1*-null (t2, t4, and t5) cell lines were plated into 96-well plates at 2,000 cells per well in 150 μL medium containing the indicated concentrations of AZD7762 or CHIR124 for 3 days. Viable cells were then counted with Dojindo's Cell Counting Kit-8 Assay. The data represent mean ± SD for three repeats. Right: GI_{50} was calculated with GraphPad. **D,** *Lkb1*-WT and *Lkb1*-null cells in six-well plates were transduced with sh*Dtymk-1*. Two sets of the cells were plated into multiple chamber slides: one was 2 days and the other was 3 days posttransduction. After overnight culturing, the cells were labeled with 100 μmol/L IdU for 20 minutes, then fixed for indirect immunofluorescence staining with anti-bromodeoxyuridine (BrdU). The data represent mean ± SD for 200 to 300 cells. **E,** representative merged images from the cells stained with IdU (red) and 4′,6-diamidino-2-phenylindole (DAPI; blue) as described in **D** are shown.

the proportion of IdU-labeled cells decreased upon *Dtymk* knockdown regardless of *Lkb1* status, although the decrease was much greater in the *Lkb1*-null cells (dropping from 43.1% to 5.8% in 3.5 days, a decrease of 86.5%) as compared with those with *Lkb1*-WT (decreasing from 57.7% to 22.3%, a decrease of 61.2%). The lower degree of labeling of *Lkb1*-null cells compared with *Lkb1*-WT cells observed under basal conditions (43.1% vs. 57.7%) may be related to the broad reductions in dNTP metabolism in *Lkb1*-null cells. After sh*Dtymk* transduction, *Lkb1*-null cells appeared normal for 3 days, but by day 4 there was massive cell death leaving virtually no surviving cells, although there was no evidence of apoptosis (data not shown). After 3.5-day knockdown of *Dtymk*, the remaining *Lkb1*-null t4 cells showed deformed and fragmented nuclei, indicative of thymineless death (Fig. 3E; refs. 24–27).

LKB1-Mutant Human NSCLC Cell Lines Are Hypersensitive to *DTYMK* Knockdown

We further sought to determine whether our observations in mouse lung cancer cells could be recapitulated in human *LKB1*-deficient NSCLC cell lines. We first screened five shRNAs targeting *DTYMK* and identified two, sh*DTYMK-D8* and sh*DTYMK-D10*, that gave efficient knockdown (Supplementary Fig. S6A and Supplementary Table S2). Next, we screened *LKB1*-WT and *LKB1*-deficient NSCLC cell lines (Fig. 4A) for proliferation in response to *DTYMK* knockdown and found that *LKB1*-deficient H2122 and A549 cell lines had heightened sensitivity as compared with *LKB1*-WT H358 and Calu-1 cell lines (Fig. 4B). Knockdown of *DTYMK* was confirmed by Western blot analysis (Fig. 4C). Sh*DTYMK*-D10 transduction showed an increased lethality in *LKB1*-WT H358 and Calu-1 cells, trending toward that of the *LKB1*-deficient cell lines (Fig. 4B). One possible explanation could involve a differential threshold of *DTYMK* knockdown, as the remaining DTYMK protein levels after sh*DTYMK*-D10 transduction were lower than those of sh*DTYMK*-D8 (Fig. 4C). This suggests that there may be a differential sensitivity to absolute DTYMK reduction between *LKB1*-deficient and *LKB1*-WT cells. DTYMK was reported to be synthetic lethal with doxorubicin in colon cancer cells independent of p53 (28). Consistently, the synthetic lethal interaction of *LKB1*-deficient and *DTYMK* knockdown may be independent of p53 status, as *LKB1*-deficient cell lines with (A549) or without (H2122) functional p53 behave similarly (Fig. 4B).

Next, we showed that knockdown of *DTYMK* in A549 cells reduced dTDP levels (Fig. 4D), suggesting that DTYMK is a major source of dTDP in human lung cancer cells. We further showed that *LKB1*-deficient cells H2122 and A549 were more sensitive than *LKB1*-WT H358 and Calu-1 cell lines to treatment with the selected CHEK1 inhibitors (Fig. 4E and Supplementary Fig. S4B), suggesting more DNA damage in *LKB1*-deficient cells than in *LKB1*-WT cell lines. This pathway seems relevant *in vivo* as *LKB1* loss was associated with elevated CHEK1 expression in *KRAS*-mutant NSCLCs (Supplementary Fig. S6B).

DISCUSSION

In the current study, we created cell lines using *Lkb1*-null lung tumor nodules and conducted multiple screens that identified *Dtymk* as a putative synthetic lethal candidate with *Lkb1* loss. Furthermore, we showed that depletion of DTYMK in mouse and human NSCLC cells diminished the dTDP pool and led to greater growth inhibition in *Lkb1/LKB1*–deficient cells; and that *LKB1* loss in mouse and human cells was linked to more DNA damage. These results suggest that DTYMK is a potential therapeutic target in *LKB1*-mutant human cancer. In addition, the parallel results observed in both mouse and human cell lines suggest that GEMM-derived tumor cell lines can be used successfully for *in vitro* synthetic lethal screening.

One possible explanation for the synthetic lethality of *Lkb1* loss and *Dtymk* knockdown is partly because of the lower expression of DTYMK in *Lkb1*-null cell lines, leading them to be more dependent on the dTTP synthesis pathway. Sh*Dtymk* depletes the absolute amount of DTYMK protein below a critical threshold, resulting in thymineless death in *Lkb1*-null cells but not in *Lkb1*-WT cells (Supplementary Fig. S7). In addition, unlike *Lkb1*-WT cell lines, *Lkb1*-null cell lines lack feedback upregulation of RPA32 expression upon *Dtymk* knockdown (Supplementary Fig. S7). Because RPA32 is involved in binding and stabilizing ssDNA during repair and replication, the lack of feedback upregulation of RPA32 expression may hinder DNA repair. A preliminary study revealed lower *Dtymk* and *Chek1* transcripts in *Lkb1*-null cell lines (Supplementary Fig. S8A and S8B), suggesting that transcriptional regulation contributes to the lower DTYMK and CHEK1 protein levels in *Lkb1*-null cell lines. More work will be needed to decipher the roles of LKB1 in the regulation of DTYMK, CHEK1, and RPA32 expression. Although *LKB1*-deficient NSCLC cell lines did not apparently show less DTYMK expression, the sh*DTYMK* data still suggested a differential sensitivity to absolute DTYMK reduction between *LKB1*-deficient and *LKB1*-WT cells. As an essential gene governing dTTP biosynthesis and DNA replication, DTYMK is necessary to all dividing cells, and overdepletion of DTYMK below the threshold is lethal to all dividing cells, especially to the tumor cells carrying low levels of deoxynucleotide pools yet maintaining a fast growth rate. This may explain the eventual death of *Lkb1/LKB1*-WT cells after *Dtymk/DTYMK* knockdown.

Human *DTYMK* was cloned by functional complementation of a *Saccharomyces cerevisiae* cell-cycle mutant *cdc8*, an essential gene for DNA synthesis (29). DTYMK is the first enzymatic step following the convergence of the *de novo* and salvage pathways in dTTP biosynthesis. In the *de novo* pathway, the DTYMK substrate dTMP is synthesized from methylation of dUMP by thymidylate synthase. In the salvage pathway, dTMP is produced from phosphorylation of thymidine by thymidine kinase. The next step in both pathways is the DTYMK-mediated phosphorylation of dTMP to form dTDP (30, 31). The production of dTDP is in contrast to that of the other deoxyribonucleotides used in DNA synthesis—dADP, dGDP, dCDP, and dUDP, which are synthesized from ADP, GDP, CDP, and UDP by ribonucleotide reductase (12, 32). Therefore, the unique dTTP biosynthesis pathway is a good target for drugs. There are multiple precedents of inhibition of the key enzymes in the *de novo* dTTP synthesis pathway, including thymidylate synthase by 5-fluorouracil or pemetrexed (15) and ribonucleotide reductase by hydroxyurea (33). We have targeted thymidylate synthase and ribonucleotide reductase in both the mouse and human

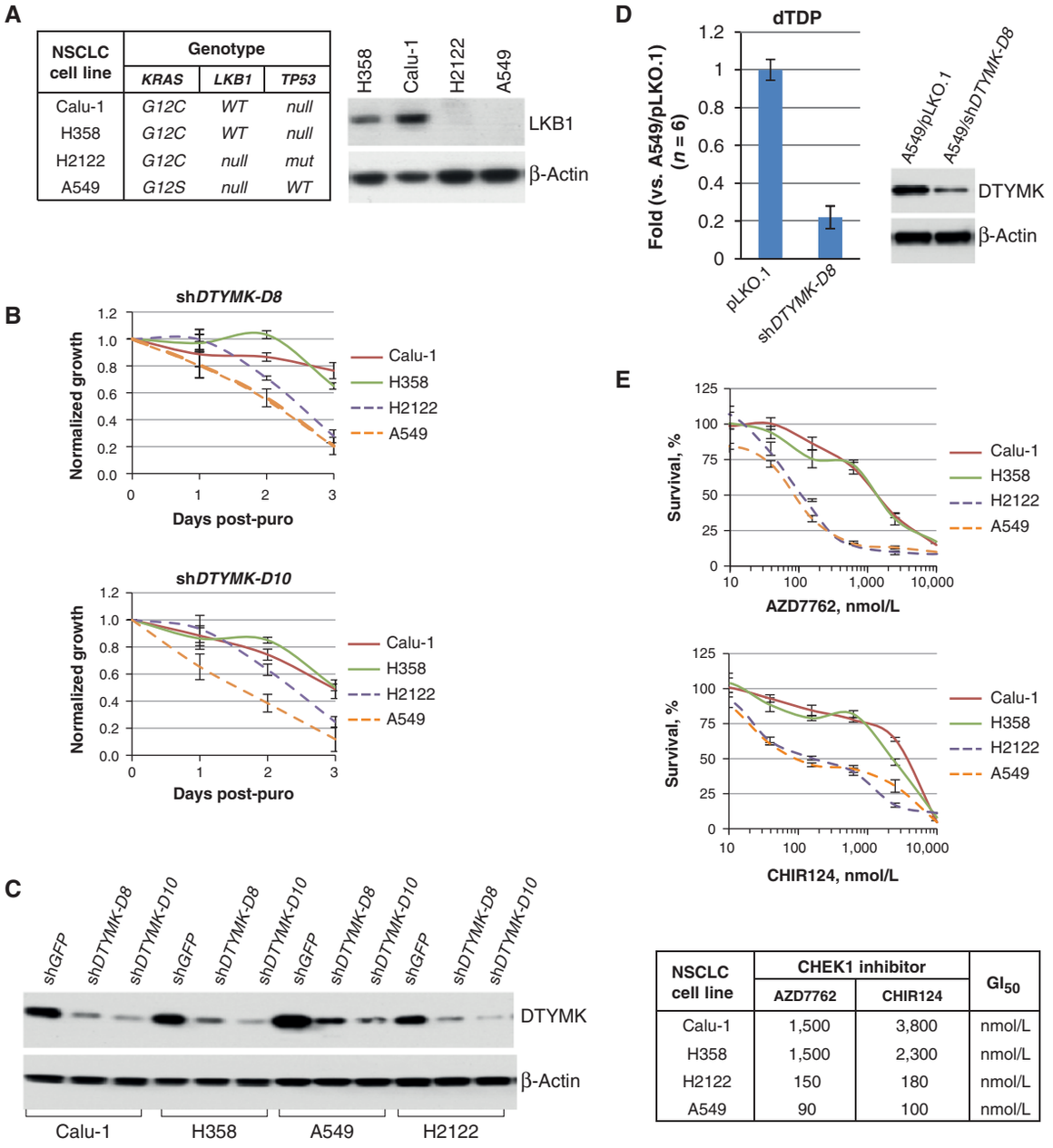

NSCLC cell line	CHEK1 inhibitor		GI_{50}
	AZD7762	CHIR124	
Calu-1	1,500	3,800	nmol/L
H358	1,500	2,300	nmol/L
H2122	150	180	nmol/L
A549	90	100	nmol/L

Figure 4. Knockdown of *DTYMK* in *LKB1*-WT and *LKB1*-mutant NSCLC cell lines. **A,** Western blot analyses of LKB1 expression in *LKB1*-WT (H358 and Calu-1) and *LKB1*-deficient (H2122 and A549) NSCLC cell lines. **B,** *LKB1*-WT (H358 and Calu-1) and *LKB1*-deficient (H2122 and A549) NSCLC cell lines were transduced with the indicated shRNAs for 1 day and then selected with 5 μg/mL puromycin (puro) for 2 days in six-well plates. The cells were collected by trypsin and replated into 96-well plates at 2,000 cells per well in 150 μL medium containing 5 μg/mL puromycin and measured daily using Promega's CellTiter-Glo Assay. The data represent mean ± SD for three replicates. **C,** the cells left from the replating were lysed for Western blot analysis of DTYMK expression. **D,** graph of dTDP levels in A549 cells transduced with the indicated shRNA for 4 days. The data represent mean ± SD for six replicates. Expression of DTYMK in these cells at the time of metabolite extraction was determined by Western blotting. **E,** *LKB1*-WT (H358 and Calu-1) and *LKB1*-deficient (H2122 and A549) NSCLC cell lines were plated into 96-well plates at 2,000 cells per well in 150 μL medium containing the indicated concentrations of AZD7762 or CHIR124 for 3 days. Viable cells were counted daily using Dojindo's Cell Counting Kit-8 Assay. The data represent mean ± SD for three repeats. Bottom: GI_{50} was calculated with GraphPad.

NSCLC *Lkb1/LKB1*-mutant cell lines using the same drugs and have not seen any selective effect on *Lkb1/LKB1*–deficient cell growth, likely because of an escape mechanism from the salvage pathway (Supplementary Fig. S9). In summary, the lack of redundant pathways for dTTP biosynthesis and the vital role of DTYMK in this process together make DTYMK a new anticancer target. In this regard, expression of *DTYMK* is increased in the majority of lung adenocarcinomas in comparison with normal lung (Supplementary Fig. S10A), and elevated *DTYMK* levels are correlated with poor survival

(Supplementary Fig. S10B). Unfortunately, *LKB1* mutation status was not determined in these datasets.

In addition to identifying DTYMK as a potential therapeutic target for *LKB1*-deficient lung cancer, we have also provided proof-of-principle that GEMM-derived cancer cell lines can provide a genetically homogeneous and therefore tractable substrate for high-throughput screens to identify novel therapeutic targets. To date, the weakness of genome-wide RNAi screening has been high false discovery rates and cell line–specific off-target effects, and consequently, despite the implementation of multiple very large-scale cell line screening programs, few actionable genotype-associated sensitivities have been uncovered to date. Our study suggests that integrating RNAi screening with metabolite profiling is an effective strategy to leverage the strengths and mitigate the weaknesses of each approach. We propose that this approach will have broad applicability, and enable more rapid development of additional targeted therapeutics for an array of genetic abnormalities occurring in cancer.

METHODS

Detailed protocols for all sections are described in the Supplementary Methods.

RNAi Screening and Metabolite Profiling

Large-scale pooled screening and data analysis were conducted at the Broad Institute's RNAi Platform as recommended previously (34), and metabolite extraction and targeted mass spectrometry analysis were conducted as reported previously (35, 36).

Cell Lines and Cell Culture

Fresh murine lung tumor nodules were minced and cultured in 100-mm dishes with RPMI-1640/10% FBS/1% penicillin–streptomycin. Calu-1, H358, H2122, and A549 (obtained from American Type Culture Collection) were cultured in RPMI-1640/10% FBS/1% penicillin–streptomycin; and 293ft (Invitrogen) was cultured in Dulbecco's Modified Eagle Medium (DMEM)/10% FBS/1% penicillin–streptomycin. All cells were cultured at 37°C in a humidified incubator with 5% CO_2.

Plasmid Constructs and Mutagenesis

pLKO.1–shRNAs were purchased from the Broad Institute (Cambridge, MA). DTYMK (BC030178) cDNAs were purchased from Thermo Scientific. shRNA-resistant DTYMKs were made by mutagenesis PCR and subcloned into the *Bam*HI and *Xho*I sites of pLenti6 vector (Invitrogen). All mutagenized cDNAs were confirmed by sequencing.

Multiple Routine In Vitro *Studies*

Lentiviral production and target cell transduction, proliferation assay, quantitative real-time PCR, Western blot analysis, flow cytometry, and immunofluorescence microscopy were conducted as described in the Supplementary Methods.

In Vivo *Study*

Lkb1-WT and *Lkb1*-null cells were transduced with pTetOn-sh*GFP* (puromycin) or pTetOn-sh*Dtymk-3* (puromycin), and then 1 million puromycin-resistant cells per transduction were implanted into athymic nude mice. When tumors grew to a diameter of 3 mm, the mice were maintained on doxycycline diet for 3 weeks to allow 634/shGFP tumors reach about 1,000 mm^3.

Disclosure of Potential Conflicts of Interest

K. Marks is employed as Associate Director at Agios Pharmaceuticals and has ownership interest (including patents) in the same. E.M. Driggers has commercial research support from Agios Pharmaceuticals. P.A. Janne has received commercial research grants from Pfizer, Boehringer Ingelheim, Sanofi-Aventis, AstraZeneca, Roche, and Genentech. J.A. Engelman has ownership interest (including patents) in Agios Pharmaceuticals and is a consultant/advisory board member of the same. R. Scully has ownership interest (including patents) in Dana-Farber Cancer Institute. A. Kimmelman is a consultant/advisory board member of Forma Therapeutics. L.C. Cantley is on the Board of Directors of Agios Pharmaceuticals, has ownership interest (including patents) in Agios Pharmaceuticals, and is a consultant/advisory board member of the same. K.-K. Wong has commercial research support from Millennium, AstraZeneca, and Infinity, has ownership interest (including patents) in G1 Therapeutics, and is a consultant/advisory board member of MolecularMD. No potential conflicts of interest were disclosed by the other authors.

The Editor-in-Chief of *Cancer Discovery* (Lewis C. Cantley) is an author of this article. In keeping with the AACR's Editorial Policy, the article was peer reviewed and a member of the AACR's Publications Committee rendered the decision about acceptability.

Authors' Contributions

Conception and design: Y. Liu, K. Marks, G.S. Cowley, P. Gao, Z. Chen, N.E. Sharpless, N. Bardeesy, R. Scully, A.L. Kung, N.S. Gray, D.E. Root, L.C. Cantley, K.-K. Wong

Development of methodology: Y. Liu, G.S. Cowley, T.J.F. Nieland, T.J. Cohoon, E.M. Driggers, J. Zhang, N. Bardeesy, J.M. Asara, L.A. Byers, A.L. Kung, D.E. Root, K.-K. Wong

Acquisition of data (provided animals, acquired and managed patients, provided facilities, etc.): Y. Liu, K. Marks, G.S. Cowley, T.J.F. Nieland, C. Xu, T.J. Cohoon, P. Gao, Y. Zhang, Z. Chen, A.B. Altabef, J.H. Tchaicha, X. Wang, E.M. Driggers, J. Zhang, S.T. Bailey, D.N. Hayes, N.M. Patel, P.A. Janne, J.M. Asara, R. Scully, L.A. Byers, D.L. Gibbons, I.I. Wistuba, J.V. Heymach, W.Y. Kim, A.L. Kung, N.S. Gray, D.E. Root, K.-K. Wong

Analysis and interpretation of data (e.g., statistical analysis, biostatistics, computational analysis): Y. Liu, K. Marks, G.S. Cowley, J. Carretero, Q. Liu, T.J.F. Nieland, Z. Chen, J.H. Tchaicha, S. Choe, E.M. Driggers, J. Zhang, N.E. Sharpless, D.N. Hayes, N. Bardeesy, J.A. Engelman, B.D. Manning, R.J. Shaw, J.M. Asara, R. Scully, A. Kimmelman, L.A. Byers, D.L. Gibbons, J.V. Heymach, D.J. Kwiatkowski, A.L. Kung, D.E. Root, K.-K. Wong

Writing, review, and/or revision of the manuscript: Y. Liu, K. Marks, Q. Liu, T.J. Cohoon, Z. Chen, E.M. Driggers, N.E. Sharpless, D.N. Hayes, P.A. Janne, N. Bardeesy, J.A. Engelman, R.J. Shaw, R. Scully, A. Kimmelman, L.A. Byers, I.I. Wistuba, J.V. Heymach, D.J. Kwiatkowski, W.Y. Kim, A.L. Kung, N.S. Gray, L.C. Cantley, K.-K. Wong

Administrative, technical, or material support (i.e., reporting or organizing data, constructing databases): Y. Liu, Q. Liu, X. Wang, J. Zhang, D.N. Hayes, K.-K. Wong

Study supervision: Y. Liu, R. Scully, A.L. Kung, K.-K. Wong

Acknowledgments

The authors thank Ozan Alkan for helping with the RNAi screen; Hin-Koon Woo, Min Yuan, and Susanne Breitkopf for conducting mass spectrometry; and Jacob B. Reibel for proofreading.

Grant Support

This work is supported by the NIH (CA122794, CA140594, CA163896, CA166480, CA154303, and Lung SPORE P50CA090578), United against Lung Cancer Foundation, American Lung Association, and Susan Spooner Research Fund (to K.-K. Wong); and by NIH

CA142794 as well as the Damon Runyon Cancer Research Foundation (to W.Y. Kim).

Received January 10, 2013; revised May 13, 2013; accepted May 13, 2013; published OnlineFirst May 28, 2013.

REFERENCES

1. Wodarz A, Nathke I. Cell polarity in development and cancer. Nat Cell Biol 2007;9:1016–24.
2. Mihaylova MM, Shaw RJ. The AMPK signalling pathway coordinates cell growth, autophagy and metabolism. Nat Cell Biol 2011;13:1016–23.
3. Vander Heiden MG, Cantley LC, Thompson CB. Understanding the Warburg effect: the metabolic requirements of cell proliferation. Science 2009;324:1029–33.
4. Gurumurthy S, Xie SZ, Alagesan B, Kim J, Yusuf RZ, Saez B, et al. The Lkb1 metabolic sensor maintains haematopoietic stem cell survival. Nature 2010;468:659–63.
5. Jones RG, Thompson CB. Tumor suppressors and cell metabolism: a recipe for cancer growth. Genes Dev 2009;23:537–48.
6. Ji H, Ramsey MR, Hayes DN, Fan C, McNamara K, Kozlowski P, et al. LKB1 modulates lung cancer differentiation and metastasis. Nature 2007;448:807–10.
7. Wingo SN, Gallardo TD, Akbay EA, Liang MC, Contreras CM, Boren T, et al. Somatic LKB1 mutations promote cervical cancer progression. PLoS ONE 2009;4:e5137.
8. Liu W, Monahan KB, Pfefferle AD, Shimamura T, Sorrentino J, Chan KT, et al. LKB1/STK11 inactivation leads to expansion of a prometastatic tumor subpopulation in melanoma. Cancer Cell 2012;21:751–64.
9. Garnett MJ, Edelman EJ, Heidorn SJ, Greenman CD, Dastur A, Lau KW, et al. Systematic identification of genomic markers of drug sensitivity in cancer cells. Nature 2012;483:570–5.
10. Mogi A, Kuwano H. TP53 mutations in nonsmall cell lung cancer. J Biomed Biotechnol 2011;2011:583929.
11. Jansen M, Ten Klooster JP, Offerhaus GJ, Clevers H. LKB1 and AMPK family signaling: the intimate link between cell polarity and energy metabolism. Physiol Rev 2009;89:777–98.
12. Su JY, Sclafani RA. Molecular cloning and expression of the human deoxythymidylate kinase gene in yeast. Nucleic Acids Res 1991;19: 823–7.
13. Van Rompay AR, Johansson M, Karlsson A. Phosphorylation of deoxycytidine analog monophosphates by UMP-CMP kinase: molecular characterization of the human enzyme. Mol Pharmacol 1999;56:562–9.
14. Taricani L, Shanahan F, Pierce RH, Guzi TJ, Parry D. Phenotypic enhancement of thymidylate synthetase pathway inhibitors following ablation of Neil1 DNA glycosylase/lyase. Cell Cycle 2010;9:4876–83.
15. Van Triest B, Pinedo HM, Giaccone G, Peters GJ. Downstream molecular determinants of response to 5-fluorouracil and antifolate thymidylate synthase inhibitors. Ann Oncol 2000;11:385–91.
16. Marenstein DR, Wilson DM, Teebor GW. Human AP endonuclease (APE1) demonstrates endonucleolytic activity against AP sites in single-stranded DNA. DNA Rep 2004;3:527–33.
17. Pogribny IP, Muskhelishvili L, Miller BJ, James SJ. Presence and consequence of uracil in preneoplastic DNA from folate/methyl-deficient rats. Carcinogenesis 1997;18:2071–6.
18. Hu CM, Yeh MT, Tsao N, Chen CW, Gao QZ, Chang CY, et al. Tumor cells require thymidylate kinase to prevent dUTP incorporation during DNA repair. Cancer Cell 2012;22:36–50.
19. Lossaint G, Besnard E, Fisher D, Piette J, Dulic V. Chk1 is dispensable for G_2 arrest in response to sustained DNA damage when the ATM/p53/p21 pathway is functional. Oncogene 2011;30:4261–74.
20. Koniaras K, Cuddihy AR, Christopoulos H, Hogg A, O'Connell MJ. Inhibition of Chk1-dependent G_2 DNA damage checkpoint radiosensitizes p53 mutant human cells. Oncogene 2001;20:7453–63.
21. Tse AN, Rendahl KG, Sheikh T, Cheema H, Aardalen K, Embry M, et al. CHIR-124, a novel potent inhibitor of Chk1, potentiates the cytotoxicity of topoisomerase I poisons *in vitro* and *in vivo*. Clin Cancer Res 2007;13:591–602.
22. Zabludoff SD, Deng C, Grondine MR, Sheehy AM, Ashwell S, Caleb BL, et al. AZD7762, a novel checkpoint kinase inhibitor, drives checkpoint abrogation and potentiates DNA-targeted therapies. Mol Cancer Ther 2008;7:2955–66.
23. Friedberg EC. How nucleotide excision repair protects against cancer. Nat Rev Cancer 2001;1:22–33.
24. Sanchez-Cespedes M, Parrella P, Esteller M, Nomoto S, Trink B, Engles JM, et al. Inactivation of LKB1/STK11 is a common event in adenocarcinomas of the lung. Cancer Res 2002;62:3659–62.
25. Knock E, Deng L, Wu Q, Lawrance AK, Wang XL, Rozen R. Strain differences in mice highlight the role of DNA damage in neoplasia induced by low dietary folate. J Nutr 2008;138:653–8.
26. Fonville NC, Vaksman Z, DeNapoli J, Hastings PJ, Rosenberg SM. Pathways of resistance to thymineless death in *Escherichia coli* and the function of UvrD. Genetics 2011;189:23–36.
27. Kuong KJ, Kuzminov A. Disintegration of nascent replication bubbles during thymine starvation triggers RecA- and RecBCD-dependent replication origin destruction. J Biol Chem 2012;287:23958–70.
28. Hu CM, Chang ZF. Synthetic lethality by lentiviral short hairpin RNA silencing of thymidylate kinase and doxorubicin in colon cancer cells regardless of the p53 status. Cancer Res 2008;68:2831–40.
29. Huang SH, Tang A, Drisco B, Zhang SQ, Seeger R, Li C, et al. Human dTMP kinase: gene expression and enzymatic activity coinciding with cell cycle progression and cell growth. DNA Cell Biol 1994;13:461–71.
30. Reichard P. Interactions between deoxyribonucleotide and DNA synthesis. Annu Rev Biochem 1988;57:349–74.
31. Arner ES, Eriksson S. Mammalian deoxyribonucleoside kinases. Pharmacol Ther 1995;67:155–86.
32. Elledge SJ, Zhou Z, Allen JB. Ribonucleotide reductase: regulation, regulation, regulation. Trends Biochem Sci 1992;17:119–23.
33. Ahmad SI, Kirk SH, Eisenstark A. Thymine metabolism and thymineless death in prokaryotes and eukaryotes. Annu Rev Microbiol 1998;52:591–625.
34. Luo B, Cheung HW, Subramanian A, Sharifnia T, Okamoto M, Yang X, et al. Highly parallel identification of essential genes in cancer cells. Proc Natl Acad Sci U S A 2008;105:20380–5.
35. Yuan M, Breitkopf SB, Yang X, Asara JM. A positive/negative ion-switching, targeted mass spectrometry-based metabolomics platform for bodily fluids, cells, and fresh and fixed tissue. Nat Protoc 2012;7:872–81.
36. Fuhrer T, Heer D, Begemann B, Zamboni N. High-throughput, accurate mass metabolome profiling of cellular extracts by flow injection-time-of-flight mass spectrometry. Anal Chem 2011;83:7074–80.